Hindawi
International Journal of Antennas and Propagation
Volume 2020, Article ID 8891759, 9 pages
https://doi.org/10.1155/2020/8891759

Research Article

Development of a Pin Diode-Based Beam-Switching Single-Layer Reflectarray Antenna

Muhammad Inam Abbasi,[1] **Muhammad Yusof Ismail**,[2] **and Muhammad Ramlee Kamarudin**[2]

[1]*Centre for Telecommunication Research & Innovation (CETRI), Faculty of Electrical and Electronic Engineering Technology (FTKEE), Universiti Teknikal Malaysia Melaka (UTeM), Melaka 76100, Malaysia*
[2]*Universiti Tun Hussein Onn Malaysia (UTHM), 86400 Batu Pahat, Johor, Malaysia*

Correspondence should be addressed to Muhammad Inam Abbasi; muhammad_inamabbasi@yahoo.com

Received 7 September 2020; Revised 13 October 2020; Accepted 13 December 2020; Published 29 December 2020

Academic Editor: Lei Yu

This paper presents a practical demonstration for the design and development of a switchable planar reflectarray using PIN diodes in the X-band frequency range. Waveguide scattering parameter measurements for the unit cells and far-field measurements of the periodic reflectarrays have been carried out to verify the predicted results. Reflectarray unit cell measurements demonstrated a frequency tunability of 0.36 GHz with a dynamic phase range of 226°. On the other hand, the designed 6×6 periodic reflectarray has been shown to achieve beam switching from +6° to −6° with different switching states of PIN diodes. This type of beam switching can be used in satellite communication for specific region coverage.

1. Introduction

Reflectarray is principally a planar reflector which consists of an array of resonant microstrip patch elements printed on a dielectric substrate and is illuminated by a feed horn. Reflectarrays offer the simplicity and high gain associated with their reflector counterparts, while providing fast, adaptive beam-forming capabilities of phased arrays at the same time. On the other hand, limited bandwidth and higher loss are some of the major drawbacks of reflectarrays that limit their use in many applications, as discussed in [1–5].

The design of beam-forming or beam-switching reflectarray depends on the reflectarray configuration where the reflected phase from each of the resonant elements can be controlled either mechanically or electronically. The reflected beam can be directed in the desired direction, which makes a reflectarray capable of achieving a wide-angle electronic beam scanning. Such a beam-forming approach can have many advantages over traditional tunable antenna array architectures, including a significant reduction in hardware required per element and increased efficiency [6]. Researchers have investigated different techniques for beam steering antennas such as the use of nonlinear dielectric materials [7–9], the integration of Radio Frequency Microelectro Mechanical Systems (RF MEMS) as switches [10, 11], loading varactor diodes with the patch elements and varying the varactor capacitance by using various biasing [12, 13], using aperture coupled elements where the tuning circuit can be located on the nonresonating surface of the element in order to control the contributed phase from each element [14], and using mechanical movement of the antenna [15]. Some other researchers have also proposed the use of PIN diodes for beam switching where the diodes can be switched ON and OFF using an external biasing circuit, and hence, the reflectarray beam can be controlled [16–19]. However, most of these works propose complex multilayer design topology using various dielectric substrates.

This work presents the design and analysis of switchable reflectarrays for beam shaping realization with optimum reflection loss and enhanced bandwidth performance. PIN

diodes have been used for beam switching in reflectarrays demonstrated through simulations and measurements of unit cells, as well as periodic arrays. The reflectarray unit cells comprise of an optimum performance single layer structure having printed patch elements with incorporated slot and gap configurations. The proposed design demonstrates a simple structure with reduced chances of mutual coupling between the adjacent elements of reflectarray.

2. Frequency Switchable Reflectarray Unit Cells

Reflectarray unit cells were designed in the X-band frequency range using Rogers Rt/D 5880 ($\varepsilon_r = 2.2$, $\tan\delta = 0.0009$), and PIN diodes were integrated into the gap introduced on the slot embedded patch element, as shown in Figure 1(a). The detailed design configuration and analysis of the rectangular slot embedded patch elements have already been presented by in [20]. Waveguide scattering parameter measurements [21] were carried out for a unit cell that comprised of two patch elements with dimensions of $L_p \times W_p = 9.4\,\text{mm} \times 10\,\text{mm}$ each, which were printed on a substrate of $L_s \times W_s = 15\,\text{mm} \times 30\,\text{mm}$. The slot length was kept at 0.6 mm, while the width was $0.5W_p$. The vertical gap was introduced with a 0.6 mm width in order to fit the PIN diode.

For the electronic switching of a PIN diode-based design, a GaAS MA4GP907 PIN diode manufactured by MACOM was used. This PIN diode has a series capacitance of 0.025pF and low series resistance of 4.2 Ω. The PIN diodes were soldered on the surface of the patch element and were powered by a power supply using a biasing circuit. 1.33 V were supplied, and a 100 Ω resistor was used. RF choke was implemented using quarter-wavelength segments and radial stub on the biasing circuit in order to block RF from reaching to the power supply. DC block capacitors were not required in this case because there is no physical connection between the RF source (network analyzer) and DC source (power supply). Figure 1(b) shows the fabricated unit cells and complete setup for frequency switchable reflectarray unit cell scattering parameter measurements.

Reflection loss and the reflection phase were measured within an X-band frequency range, and a close agreement between measured and simulated results was observed. Figure 2(a) shows a comparison between measured and simulated reflection loss curves for fabricated samples. It can be observed from Figure 2(a) that, in the OFF state of PIN diode, the measured resonant frequency is close to the simulated resonant frequency. The fabricated unit cell resonated at 9.40 GHz with a reflection loss of 2.60 dB, while the simulations for OFF state of PIN diode provided a resonant frequency of 9.38 GHz with 1.61 dB reflection loss. When the PIN diodes were switched ON, a clear change in frequency was observed for the fabricated samples. In the ON state, the measured resonant frequency was observed to be 9.04 GHz with reflection losses of 3.91 dB. At the same time, the simulation results for the ON state of the PIN diode exhibited a reflection loss of 2.88 dB at a resonant frequency of 8.99 GHz. The maximum discrepancy between measured and simulated reflection loss was observed to be 0.99 dB and 1.03 dB in OFF and ON states of PIN diodes, respectively. Moreover, extra noise or ripples with a maximum level of 0.25 dB were observed. The reason for this discrepancy can be fabrication quality, which may be affected by the soldering of diodes and photoetching process, as well as the difference between actual material properties and the properties given in the datasheet. Figure 2(b) shows the comparison between the measured and simulated reflection phase. A close agreement between the measured and simulated phase can be observed in Figure 2(b) except the ripples found towards the edges of the measured curves. These ripples can be linked to the same sources, which caused a discrepancy in the reflection loss curves. As shown in Figure 2(a), the dynamic phase range ($\Delta\varphi_d$) was calculated at the central frequency of two resonant curves in OFF and ON states of PIN diodes. It can be observed from that a maximum frequency tunability of 0.36 GHz and a dynamic phase range of 226° were demonstrated by the PIN diode-based unit cell measurements. The results are in close agreement with the results obtained by 3D EM simulators of CST MWS and Ansoft HFSS, which practically validates the proposed design.

3. Switchable Periodic Reflectarray Design

After the characterization of the reflectarray unit cells and the achievement of the required progressive phase distribution, switchable periodic reflectarrays were designed. In order to design the periodic arrays, a mathematical model has been developed which guides to the exact placement of the unit cells in the array environment. The developed mathematical model has then been applied to design the periodic arrays and perform the far-field measurements. The following sections will explain the procedure and result in details.

3.1. Mathematical Modelling for the Periodic Reflectarray Design. In order to design a reflectarray antenna, the most imperative scrutiny is the analysis of the total electric field on the patch elements printed on the dielectric substrate with a conductive ground plane on the other side. The total electric field on a reflectarray consists of the incident field and the reflected and scattered elements of the field. Therefore, the total electric field can be given by

$$\overline{E}_t = \left[1 + \overline{\overline{R}}(\theta_i, \varphi_i) + \overline{\overline{S}}(\theta_i, \varphi_i, L_i, W_i)\right] \cdot \overline{E}_0 e^{jk_0\left(xu_i + yv_i - z\cos\theta_i\right)}. \tag{1}$$

In the case of a waveguide simulator technique, the general relation for the total electric field excited in the Y-direction can be written as

$$\overline{E}_{tw} = \overline{\overline{G}}_{YY} \cdot \overline{J}_Y + \overline{E}_{Yinc}\left(l + \overline{\overline{G}}_{YY}\right), \tag{2}$$

where $\overline{\overline{G}}$ is Green's function, $\overline{J}$ is the current density, and l is the length of the unit cell patch element, and $\overline{J}_Y$ can be given by

$$\overline{J}_Y = \sum_n A_n \varphi_n(x, y), \tag{3}$$

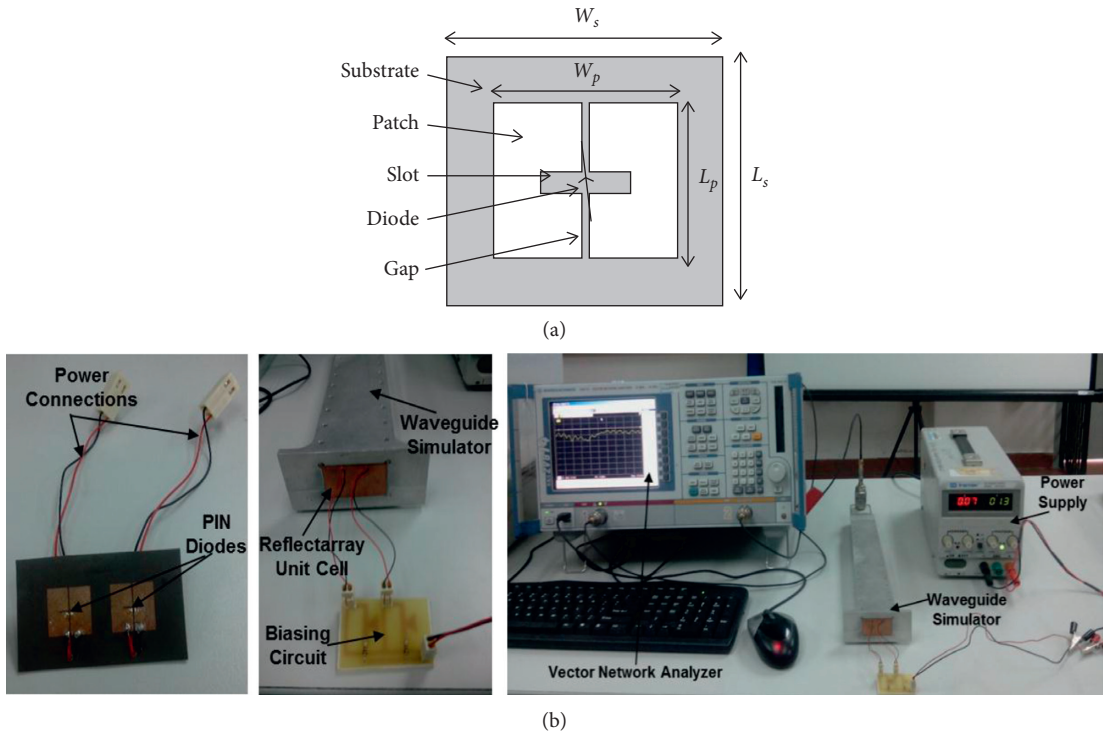

FIGURE 1: Reflectarray unit cell. (a) Proposed design configuration. (b) Fabricated unit cell, biasing circuit, and complete measurements setup.

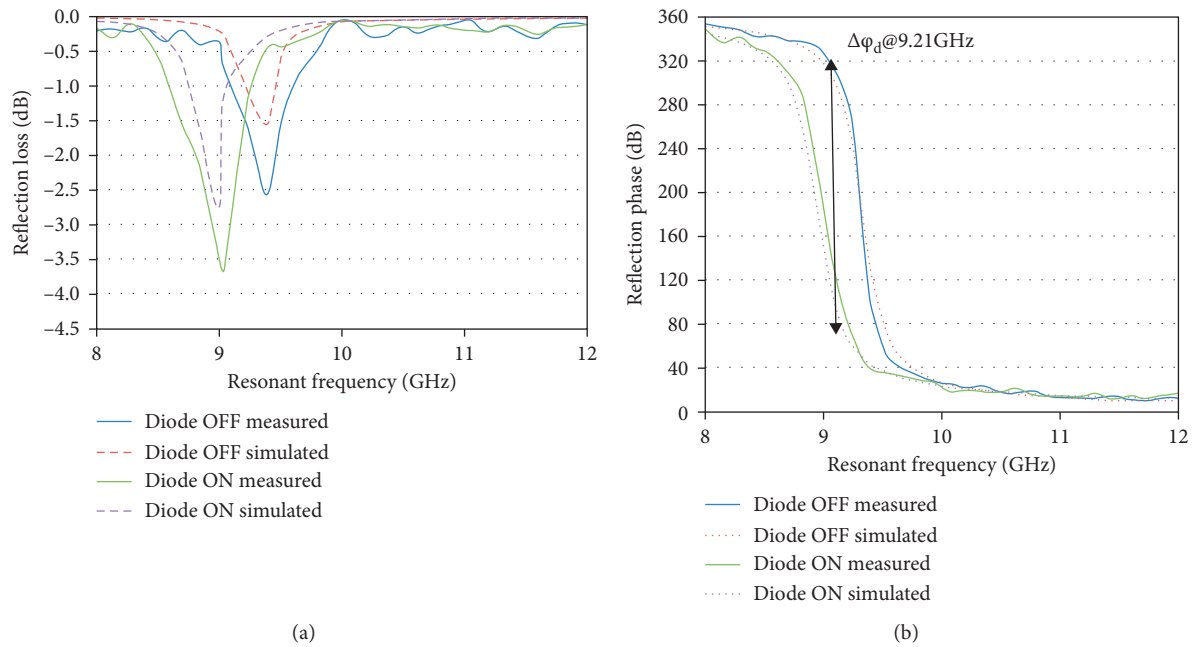

FIGURE 2: PIN diode-based active unit cells of reflectarrays. (a) Measured and simulated reflection loss curves. (b) Measured and simulated reflection phase curves.

where A_n is the unknown vector coefficient and φ_n is the required phase from an individual patch element of a reflectarray in order to form a progressive phase distribution.

In order to calculate the phase shift for the elements on the X-axis, trigonometric identities can be used as follows:

$$\varphi = -\frac{2\pi}{3}\cot^{-1}\frac{f}{x_i \pm \Delta X}, \tag{4}$$

where f is the vertical distance of feed from the surface of the array and x_i is the distance between the center of the ith

element and the point perpendicular to the feed and φ is in degrees. Once φ is calculated for different values of $x = x_i$, $y = 0$, the phase shift for all the array elements can be obtained. This method simplifies the calculation of the required phase shift from each of the array elements and reduces the complexity and time required for the periodic reflectarray design. The abovementioned technique can also be used for the progressive phase distribution with offset feed reflectarrays as shown in Figure 3. In the case of offset feed reflectarrays, ΔX has to be introduced as the distance between the feed and the line perpendicular to the array centre. Figure 3 shows the geometry of the centre feed and offset feed reflectarrays for different planar reflector designs. The feeds F1 and F2 are placed at the offset distance of $\Delta X = X_0 - X_2$and $\Delta X = X_0 - X_2$, respectively.

The abovementioned analysis provides a general formula for the design of a planar reflector with progressive phase distribution for any dielectric material and either centre or offset feed configuration. In order to obtain the progressive phase distribution of a planar reflector designed with different dielectric substrates, the material properties should be incorporated in equation (4). The material properties affect the reflection coefficient (Γ), which affects the reflection phase of the planar reflector. In the case of reflectarray antennas, Γ depends on the attenuation due to dielectric and conductor loss, which are given by

$$\alpha_{\mathrm{d}} = \frac{\omega}{2}\sqrt{(\mu_0\epsilon_0\epsilon_r)}\tan\delta,$$
$$\alpha_{\mathrm{c}} = \frac{8.68}{WZ_m}\sqrt{\left(\frac{\omega\mu_0}{2\sigma_{\mathrm{c}}}\right)}, \tag{5}$$

where α_{d} and α_{c} are attenuation due to dielectric and copper loss, respectively.

After incorporation of the effects of dielectric and copper attenuation on Γ and reflection phase of the planar reflector, equation (4) can be written as

$$\varphi = -\frac{2\pi}{3}\cot^{-1}\frac{f}{K\left(x_i \pm \Delta X_f\right)}. \tag{6}$$

In equation (6), K is a variable that relates ϕ with Γ and depends on resonant frequency and material properties, which affect the radiated and scattered fields. The value of K will be higher for the materials with higher values of dielectric permittivity and loss tangent. Therefore, K is directly proportional to attenuation due to the dielectric and conductor, and K can be given by

$$K = C \cdot (\alpha_{\mathrm{d}} + \alpha_{\mathrm{c}}), \tag{7}$$

where C is a compensation variable and varies with different design requirements and materials used. Finally, equation (6) can be written as

$$\varphi = -\frac{2\pi}{3}\cot^{-1}\frac{f}{C \cdot (\alpha_{\mathrm{d}} + \alpha_{\mathrm{c}})\left(x_i \pm \Delta X_f\right)}. \tag{8}$$

In order to implement the mathematical model for periodic arrays designed using different dielectric materials,

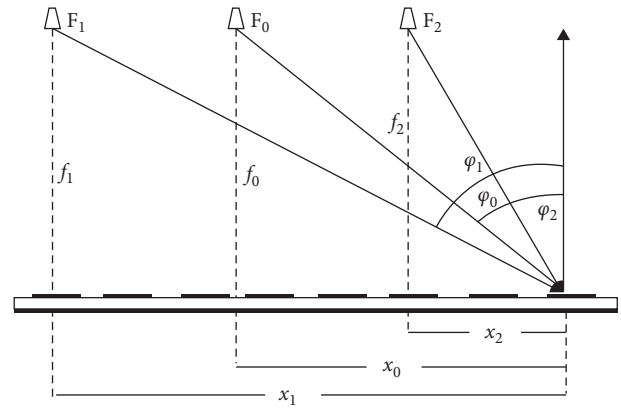

Figure 3: Reflection phase from different feed points in a planar reflector.

the compensation factor C can be expanded by relating C, with different material properties, and finally, the reflection phase of the individual elements can be given by

$$\phi = -\frac{2\pi}{3}\cot^{-1}\frac{f}{x\left(\varepsilon_r/\tan\delta\right)\left(\alpha_{\mathrm{d}} + \alpha_{\mathrm{c}}\right)\left(x_i \pm X_f\right)}, \tag{9}$$

where x is a constant that has to be derived for different materials. Values of C have been estimated as a function of material properties and the desired frequency range.

In order to demonstrate the functionality of the developed mathematical modelling, phase distribution for different offset fed reflectarrays was obtained. An offset of 0.5λ (15 mm for 10 GHz) has been used for five different feed positions placed at $f = f_0$ (centre feed), $f = f_0 - \lambda$, $f = f_0 + \lambda$, $f = f_0 - 1/2\lambda$, and $f = f_0 + 1/2\lambda$. The required reflection phases for progressive phase distribution of planar reflectors with different offset feed positions are shown in Figure 4. It can be observed from Figure 4 that a phase shift is required because of an offset in the feed position. However, for a particular design (constant number of elements and material properties), the phase values obtained by mathematical modelling for a radius of the circle are independent of the feed positions.

3.2. Array Design and Far-Field Measurements. Active arrays with a 6×6 slot and gap embedded patch elements were designed and fabricated, and the PIN diodes were incorporated on half of the resonant elements (18 diodes) for the demonstration of radiation pattern measurements of beam-switching reflectarrays. In order to achieve the progressive phase distribution using the individual unit cells of reflectarray, the phase shift was obtained by varying the width of the rectangular slots. There were no changes made in the dimensions of the gap and properties of the PIN diodes.

The PIN diodes were forward biased with a 1.33 V forward voltage and a biasing resistance of 100 Ω. Therefore, the total current demanded by the antenna was 239.4 mA. Figure 5 shows the fabricated 6×6 element reflectarray with connectors attached to it. As shown in Figure 5, the biasing circuit was used to bias the 18 PIN

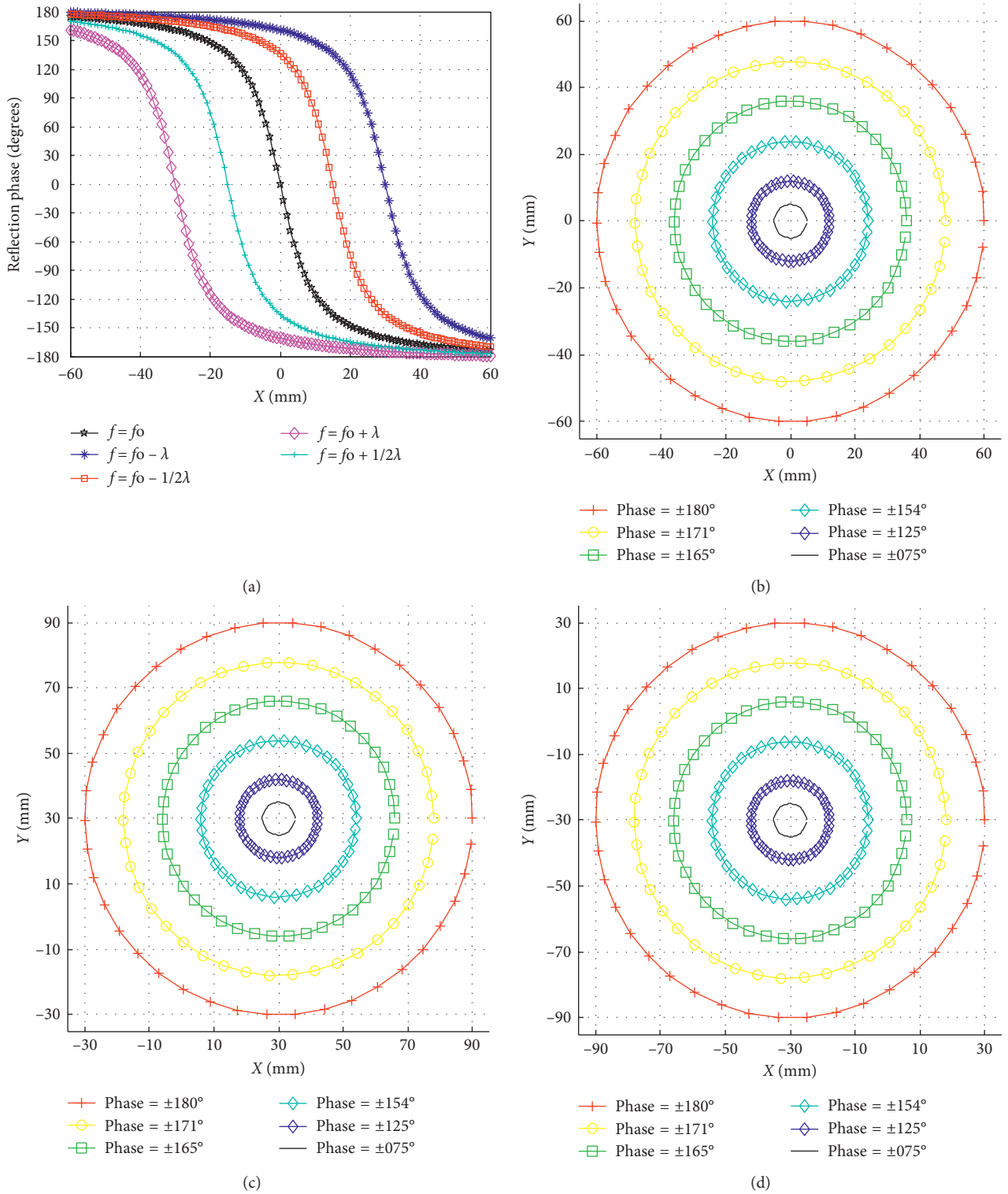

Figure 4: Continued.

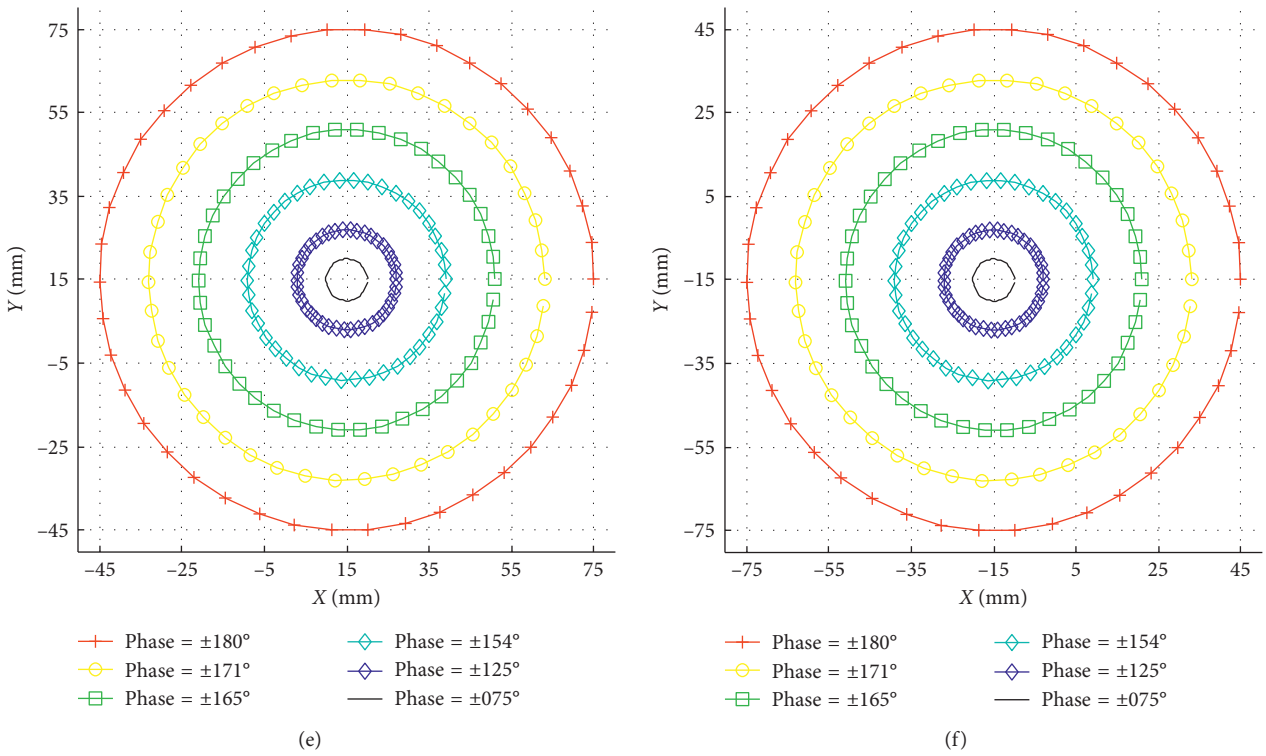

Figure 4: Required reflection phase curves for a planar reflector (8 × 8 elements) (a) with different feed positions, (b) $f = f_0$ (centre feed), (c) $f = f_0 - \lambda$, (d) $f = f_0 + \lambda$, (e) $f = f_0 - 1/2\lambda$, and (f) $f = f_0 + 1/2\lambda$.

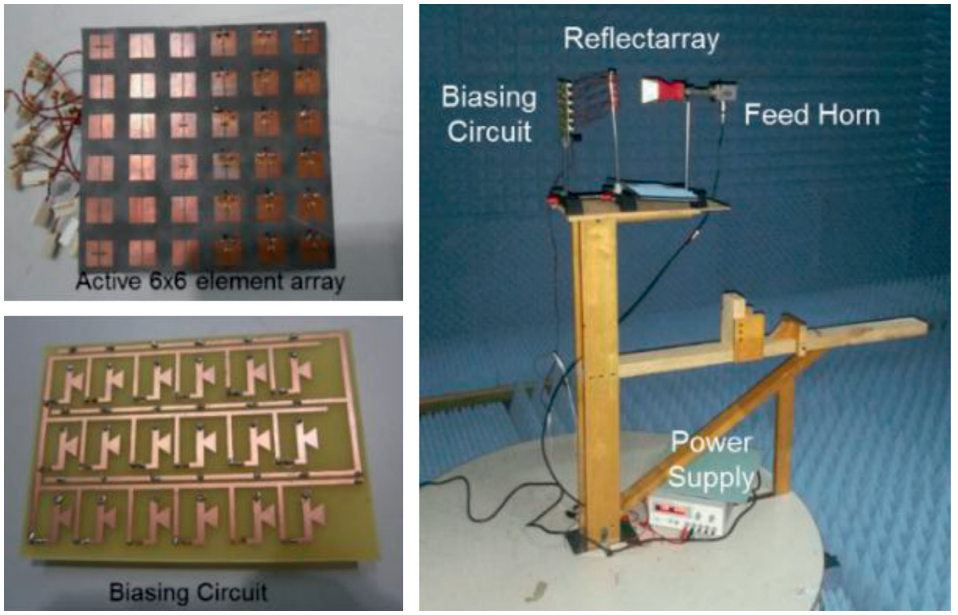

Figure 5: Fabricated 6 × 6 element active array, biasing circuit, and complete far-field measurement setup for an active reflectarray antenna.

diodes where the power was supplied using a power supply placed inside the anechoic chamber. The reflectarray antenna was placed at a far-field distance from a standard X-band transmitting horn antenna. The feed horn has a gain of around 7.5 dB at 10 GHz. The transmitter and receiver were connected with a control station and a network analyzer placed outside the chamber. A turntable was used to rotate the reflectarray antenna, and far-field measurement results were stored in the control station. A very close agreement between measured and simulated far-

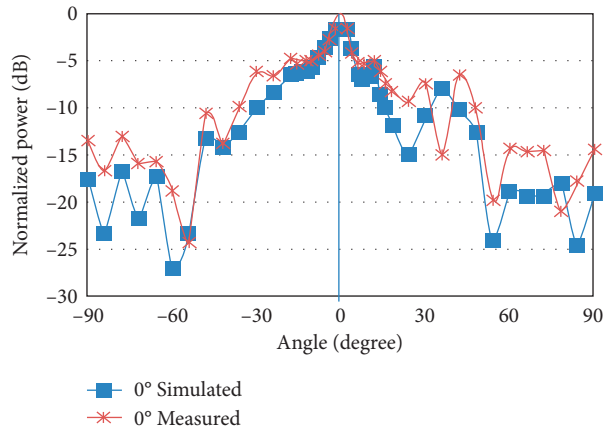

Figure 6: Measured and simulated radiation patterns for 0° primary beam at 10 GHz.

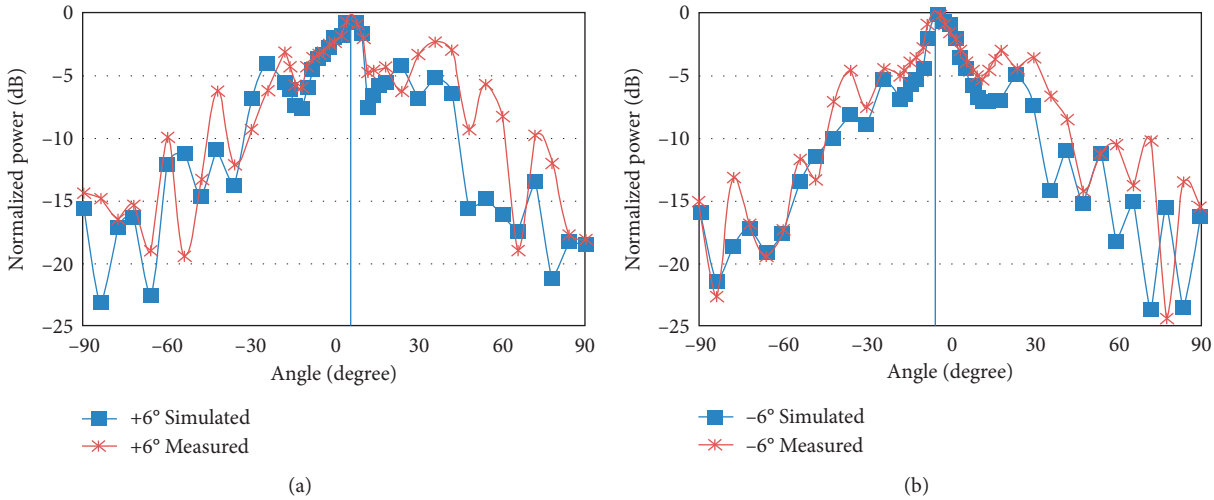

Figure 7: Measured and simulated radiation patterns of reflectarrays. (a) +6° switched beam. (b) −6° switched beam at 10 GHz.

field radiation pattern results was demonstrated where measured 3 dB beamwidth of 13.3° for 0° beam was observed as compared to 3 dB beamwidth of 12.9° generated during simulations as shown in Figure 6.

A switched beam of +6° was achieved by forward biasing (ON state) of the diodes keeping the diodes on the right side of the array. Therefore, half of the array resonant elements on the left side, without diodes, were considered to be in the OFF state of PIN diodes. In the OFF state, a PIN diode acts as an open circuit with a very low series capacitance. Keeping this in view, the assumption of elements without diodes as in the OFF state can be acceptable for demonstration purposes. A switched beam of −6° was demonstrated by changing the configuration of reflectarray in such a way that the PIN diode loaded elements were placed on the left side of the array. This was achievable because of the symmetricity of the reflectarray design and positioning of the PIN diodes. The switched beam configurations also provided a good agreement between simulated and measured results. Figure 7(a) shows a comparison between measured and simulated results for +6° switched beam configuration, where measured and simulated 3 dB beamwidth were observed to be 13.2° and 13.8°, respectively. While for −6°, switched beam measured 3 dB beamwidth was observed to be 13.3° as compared to the simulated 3 dB beamwidth of 14.0° as shown in Figure 7(b). The maximum discrepancy in the case of active reflectarray antenna design was observed to be 0.7°; however, the trend of beam switching for measured radiation patterns is similar to the simulated radiation patterns. Moreover the cross polarization levels were observed to be below −20 dB which are considered satisfactory for this type of antenna.

The comparison between the measured and simulated antenna gains was also carried out as shown in Table 1. A maximum gain of 13 dB was observed in the case of 0° beam. The gain was observed to be slightly lower in the case of switched beams which can be due to the effects caused by the introduction of PIN diodes. The −1 dB gain bandwidth was also obtained for the 0° beam by measuring the gain at different frequencies and observing the bandwidth at 1 dB

Table 1: Comparison between simulated and measured gain values at 10 GHz.

Beam	Simulated gain (dB)	Measured gain (dB)
0°	13.0	12.72
+6°	12.8	12.62
−6°	12.8	12.58

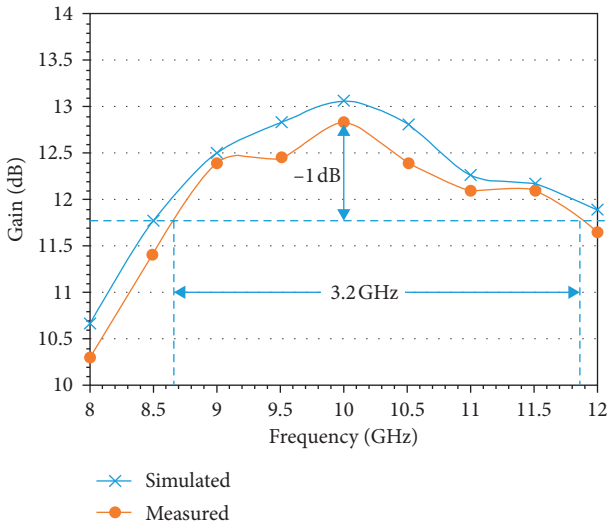

Figure 8: Measured and simulated gain of reflectarrays of 0° beam in the X-band frequency range.

below the maximum gain at 10 GHz. Figure 8 shows the comparison between the simulated and measured results of gain at different frequencies in the X-band frequency range. The 1 dB was observed to be 32% or 3.2 GHz as demonstrated in Figure 8.

Generally, there are some discrepancies observed by the comparison of simulated and measured results of different performance parameters. The discrepancy in the measured and simulated results can mainly be attributed to the losses added because of the additional circuitry used for biasing of active reflectarrays. The PIN diodes were soldered on the resonant patch elements using conducting materials, which can add up to the conductor losses. Moreover, during the fabrication and soldering process, the arrays were exposed to very high temperatures. This high temperature can vary the material properties of the dielectric substrate, and the soldering can affect the conductivity of the copper used for resonant patches. Overall, it can be concluded that the results successfully demonstrated the feasibility of applying the developed technique for the design of switchable reflectarrays for beam-shaping realization.

4. Conclusions

Switchable reflectarrays for beam-shaping realization can be designed using PIN diodes on the slot and gap embedded resonant patch elements of reflectarrays. The performance of the unit cells and the PIN diodes has to be optimized for the effective design of active reflectarrays. Furthermore, the sidelobe levels and 3 dB beamwidth demonstrated in this work can be improved by increasing the number of elements in the periodic array. Such beam switching can be used in a number of applications, including Earth observatory systems, where a geostationary orbit can cover the whole Earth within ±9°.

Data Availability

The corresponding author can be contacted for any supporting data.

Conflicts of Interest

The authors declare that they have no conflicts of interest.

Acknowledgments

Research funding for this work was fully provided by the Ministry of Higher Education, Malaysia, under the Prototype Research Grant Scheme (PRGS, VOT 0904) and Research Acculturation Collaborative Effort (RACE, VOT 1119).

References

[1] J. Huang and J. Encinar, *Reflectarray Antennas: Broadband Techniques*, Wiley, Hoboken, NJ, USA, 2007.

[2] M. Y. Ismail and M. Inam Abbasi, "Performance improvement of reflectarrays based on embedded slots configurations," *Progress in Electromagnetics Research C*, vol. 14, pp. 67–78, 2010.

[3] M. Fazaelifar, S. Jam, and R. Basiri, "Design and fabrication of a wideband reflectarray antenna in Ku and K bands," *AEU - International Journal of Electronics and Communications*, vol. 95, pp. 304–312, 2018.

[4] G.-T. Chen, Y.-C. Jiao, and G. Zhao, "A reflectarray for generating wideband circularly polarized orbital angular momentum vortex wave," *IEEE Antennas and Wireless Propagation Letters*, vol. 18, no. 1, pp. 182–186, 2019.

[5] M. Karimipour and I. Aryanian, "Demonstration of broadband reflectarray using unit cells with spline-shaped geometry," *IEEE Transactions on Antennas and Propagation*, vol. 67, no. 6, pp. 3831–3838, 2019.

[6] S. V. Hum, M. Okoniewski, and R. J. Davies, "Realizing an electronically tunable reflectarray using varactor diode-tuned elements," *IEEE Microwave and Wireless Components Letters*, vol. 15, no. 6, pp. 422–424, 2005.

[7] M. Y. Ismail, W. Hu, R. Cahill et al., "Phase Agile reflectarray cells based on liquid crystals," *IEE Proceedings - Microwaves, Antennas and Propagation*, vol. 1, no. 4, pp. 809–814, 2007.

[8] W. Hu, M. Y. Ismail, R. Cahill et al., "Tunable liquid crystal patch element," *IET Electronic Letters*, vol. 42, no. 9, pp. 509–511, 2006.

[9] A. Mossinger, R. Marin, S. Mueller, J. Freese, and R. Jakoby, "Electronically reconfigurable reflectarrays with nematic liquid crystals," *IET Electronics Letters*, vol. 42, no. 16, pp. 899-900, 2006.

[10] H. Rajagopalan, Y. Rahmat, and W. A. Imbriale, "RF MEMES actuated reconfigurable reflectarray patch-slot element," *IEEE Transactions on Antennas and Propagation*, vol. 56, no. 12, pp. 3689–3699, 2008.

[11] F. A. Tahir, H. Aubert, and E. Girard, "Equivalent electrical circuit for designing MEMS-controlled reflectarray phase

shifters," *Progress in Electromagnetics Research*, vol. 100, pp. 1–12, 2010.

[12] L. Boccia, F. Venneri, G. Amendola, and G. D. Massa, "Application of varactor diodes for reflectarray phase control," *IEEE International Symposium of Antennas and Propagation Society*, vol. 3, pp. 132–135, 2002.

[13] S. V. Hum, M. Okoniewski, and R. Davies, "Modeling and design of electronically tunable reflectarrays," *IEEE Transactions on Antennas and Propagation*, vol. 55, no. 8, pp. 2200–2210, 2007.

[14] M. Riel and J. J. Laurin, "Design of an electronically beam scanning reflectarray using aperture-coupled elements," *IEEE Transactions on Antennas and Propagation*, vol. 55, no. 5, pp. 1260–1266, 2007.

[15] M. I. Abbasi, M. H. Dahri, M. H. Jamaluddin, N. Seman, M. R. Kamarudin, and N. H. Sulaiman, "Millimeter wave beam steering reflectarray antenna based on mechanical rotation of array," *IEEE Access*, vol. 7, pp. 145685–145691, 2019.

[16] E. Carrasco, M. Barba, and J. A. Encinar, "X-band reflectarray antenna with switching-beam using PIN diodes and gathered elements," *IEEE Transactions on Antennas and Propagation*, vol. 60, no. 12, pp. 5700–5708, 2012.

[17] H. Yang, F. Yang, S. Xu et al., "A 1-bit 10×10 reconfigurable reflectarray antenna: design, optimization, and experiment," *IEEE Transactions on Antennas and Propagation*, vol. 64, no. 6, pp. 2246–2254, 2016.

[18] J. Han, L. Li, G. Liu, Z. Wu, and Y. Shi, "A wideband 1 bit 12×12 reconfigurable beam-scanning reflectarray: design, fabrication, and measurement," *IEEE Antennas and Wireless Propagation Letters*, vol. 18, no. 6, pp. 1268–1272, 2019.

[19] H. Zhang, X. Chen, Z. Wang, Y. Ge, and J. Pu, "A 1-bit electronically reconfigurable reflectarray antenna in X band," *IEEE Access*, vol. 7, pp. 66567–66575, 2019.

[20] M. Y. Ismail and M. Inam, "Resonant Elements for Tunable Reflectarray Antenna Design," *International Journal of Antennas and Propagation*, vol. 2012, Article ID 9148686, 6 pages, 2012.

[21] M. Inam and M. Y. Ismail, "Reflection loss and bandwidth performance of X-band infinite reflectarrays: simulations and measurements," *Microwave and Optical Technology Letters*, vol. 53, no. 1, pp. 77–80, 2011.